# Guanylate Kinase 1 Deficiency: A Novel and Potentially Treatable Mitochondrial DNA Depletion/Deletions Disease

Agustin Hidalgo-Gutierrez, PhD,[1] Jonathan Shintaku,[1] Javier Ramon,[2,3] Eliana Barriocanal-Casado,[1] Alba Pesini,[1] Russell P. Saneto,[4] Gloria Garrabou,[2,5] Jose Cesar Milisenda,[2,5,6] Ana Matas-Garcia,[2,5,6] Laura Gort,[2,7] Olatz Ugarteburu,[2,7] Yue Gu,[8] Lahari Koganti,[8] Tian Wang,[9] Saba Tadesse,[1] Megi Meneri,[10,11] Monica Sciacco,[12] Shuang Wang,[9] Kurenai Tanji,[8] Marshall S. Horwitz,[13] Michael O. Dorschner,[13] Mahesh Mansukhani,[8] Giacomo Pietro Comi,[10,11] Dario Ronchi,[10,11] Ramon Marti,[2,3] Antonia Ribes,[2,7] Frederic Tort,[2,7] and Michio Hirano, MD[1]
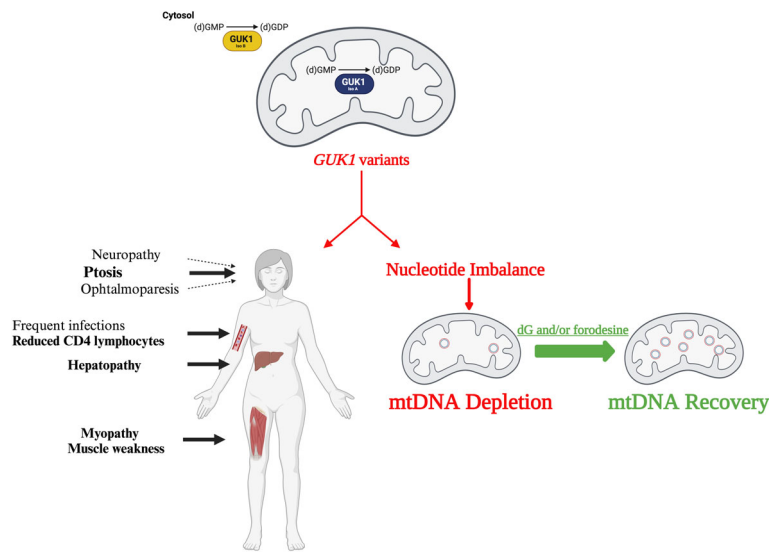
[Color figure can be viewed at www.annalsofneurology.org]

Address correspondence to Michio Hirano, Columbia University Irving Medical Center, 630 West 168th Street, P&S 4-423, New York, NY 10032. E-mail: mh29@columbia.edu

From the [1]Department of Neurology, Columbia University Irving Medical Center, New York, NY; [2]Biomedical Network Research Centre on Rare Diseases (CIBERER), Instituto de Salud Carlos III, Madrid, Spain; [3]Vall d'Hebron Research Institute, Autonomous University of Barcelona, Barcelona, Spain; [4]Seattle Children's Hospital, Seattle, WA; [5]Inherited Metabolic Diseases and Muscle Disorder's Lab, Cellex – IDIBAPS, Faculty of Medicine and Health Science – University of Barcelona (UB), Barcelona, Spain; [6]Department of Internal Medicine, Hospital Clínic of Barcelona, Barcelona, Spain; [7]Section of Inborn Errors of Metabolism-IBC, Department of Biochemistry and Molecular Genetics, Hospital Clinic de Barcelona-IDIBAPS, Barcelona, Spain; [8]Department of Pathology and Cell Biology, Columbia University Irving Medical Center, New York, NY; [9]Department of Biostatistics, Mailman School of Public Health, Columbia University, New York, NY; [10]Dino Ferrari Center, Department of Pathophysiology and Transplantation, University of Milan, Milan, Italy; [11]IRCCS Fondazione Ca' Granda Ospedale Maggiore Policlinico, Neurology Unit, Milan, Italy; [12]IRCCS Fondazione Ca' Granda Ospedale Maggiore Policlinico, Neuromuscular and Rare Disease Unit, Milan, Italy; and [13]Department of Laboratory Medicine and Pathology, University of Washington, Seattle, WA

Additional supporting information can be found in the online version of this article.

Objective: Mitochondrial DNA (mtDNA) depletion/deletions syndrome (MDDS) comprises a group of diseases caused by primary autosomal defects of mtDNA maintenance. Our objective was to study the etiology of MDDS in 4 patients who lack pathogenic variants in known genetic causes.

Methods: Whole exome sequencing of the probands was performed to identify pathogenic variants. We validated the mitochondrial defect by analyzing mtDNA, mitochondrial dNTP pools, respiratory chain activities, and GUK1 activity. To confirm pathogenicity of GUK1 deficiency, we expressed 2 GUK1 isoforms in patient cells.

Results: We identified biallelic *GUK1* pathogenic variants in all 4 probands who presented with ptosis, ophthalmoparesis, and myopathic proximal limb weakness, as well as variable hepatopathy and altered T-lymphocyte profiles. Muscle biopsies from all probands showed mtDNA depletion, deletions, or both, as well as reduced activities of mitochondrial respiratory chain enzymes. *GUK1* encodes guanylate kinase, originally identified as a cytosolic enzyme. Long and short isoforms of GUK1 exist. We observed that the long isoform is intramitochondrial and the short is cytosolic. In probands' fibroblasts, we noted decreased GUK1 activity causing unbalanced mitochondrial dNTP pools and mtDNA depletion in both replicating and quiescent fibroblasts indicating that GUK1 deficiency impairs de novo and salvage nucleotide pathways. Proband fibroblasts treated with deoxyguanosine and/or forodesine, a purine phosphatase inhibitor, ameliorated mtDNA depletion, indicating potential pharmacological therapies.

Interpretation: Primary GUK1 deficiency is a new and potentially treatable cause of MDDS. The cytosolic isoform of GUK1 may contribute to the T-lymphocyte abnormality, which has not been observed in other MDDS disorders.

Mitochondrial DNA (mtDNA) depletion/deletions syndrome (MDDS) is characterized by a substantial decrease in full-length mtDNA in one or more tissues.[1,2] Clinically, they present as myopathic, encephalomyopathic, hepatocerebral, or neurogastrointestinal disorders. The most severe forms of MDDS manifest in early childhood with multisystemic phenotypes, such as Alpers hepatocerebral syndrome, and mtDNA depletion in affected tissues. In contrast, adult-onset chronic progressive external ophthalmoplegia (CPEO) typically shows exclusively multiple deletions of mtDNA in skeletal muscle.[3,4] In many cases of MDDS, both depletion and deletions of mtDNA are detected.

Maintenance of mtDNA through high-fidelity replication and repair requires a balanced supply of deoxynucleoside triphosphates (dNTPs). The major nucleos(t)ide synthesis pathways are the de novo and the salvage pathways. In replicating cells, the cytosolic de novo pathway is upregulated due to increased dNTPs requirements for nuclear DNA (nDNA) synthesis.[5] In contrast, in postmitotic cells, the de novo pathway is suppressed, and cytosolic and mitochondrial salvage pathways are required to generate dNTPs for mtDNA replication, which occurs constitutively.[5]

Initially, autosomal recessive defects of the mitochondrial salvage pathway enzymes thymidine kinase 2 (TK2) and deoxyguanosine kinase (dGK) were linked to myopathic and hepatocerebral forms of MDDS. Subsequent identification of autosomal dominant and recessive pathogenic variants in *RRM1* and *RRM2B* subunits of ribonucleotide reductase in multisystemic and myopathic forms of MDDS has revealed the importance of the de novo pathway in mtDNA maintenance. Additional genes, such as *TYMP*, *ABAT*, and *GMPR*, are also required for dNTP pool balance and, when mutated, cause MDDS.[6–13]

Guanylate kinase, encoded by *GUK1*, is a nucleotide monophosphate kinase (NMPK) that catalyzes the phosphorylation of guanosine and deoxyguanosine monophosphates (GMP and dGMP [(d)GMP]) to guanosine and deoxyguanosine diphosphate (GDP and dGDP [(d)GDP]). Since the initial isolation of human GUK1 from erythrocytes in the 1970s,[14,15] its structure, function, and substrate specificity have been extensively studied as potential targets for antiviral and anticancer treatments.[14,16] Although subcellular localization of other NMPKs, such as adenylate kinase, which has 9 isoforms, including 3 mitochondrial isoforms,[17,18] have been studied in detail, the intracellular localization of GUK1 has not been investigated. The two major GUK1 isoforms are a 218 amino acid long isoform (hereafter isoform A) and 197 amino acid short isoform (hereafter isoform B). The cytosolic conversion of (d)GMP to (d)GDP has been attributed to GUK1 and a presumed analogous mitochondrial enzyme. Alternatively, dGDP required for proper maintenance of mtDNA may be synthesized in the cytosol by GUK1 and transported into mitochondria through purine transporters.[19–22] A third scenario invokes GUK1 as the sole enzyme responsible for this reaction in both the cytosol and mitochondria.

Here, we report a novel MDDS, in 4 probands from 3 families, due to autosomal recessive GUK1 deficiency that impairs NMPK leading to MDDS. In addition, we have identified effective in vitro therapeutic strategies to potentially treat this disorder. Our studies also reveal that the long GUK1 isoform is intra-mitochondrial, whereas the short GUK1 isoform is cytosolic.

Material and Methods

Study Approval

Informed consent for anonymous publication of patient clinical features and analyses of DNA/RNA samples, skin-derived fibroblasts, and excess clinical samples of muscle tissues were obtained from study participants under Columbia University Irving Medical Center Institutional Review Board approved protocols or with local ethics committee approval of the Hospital Clinic de Barcelona-IDIBAPS, Barcelona, Spain, or the University of Milan.

Variant Identification

Exome sequencing of the probands or trio exome sequencing was performed on peripheral blood in the routine clinical evaluation of the patients, and potential pathogenic variants as well as autosomal recessive inheritance from the healthy parents were confirmed by Sanger DNA sequencing.

Cell Culture and Cell Assays

Skin fibroblasts were obtained by punch biopsies from human controls and patients. *GUK1* pathogenic variants were confirmed by Sanger DNA sequencing. Cells were grown to promote proliferative or quiescence conditions, as previously described.[11] Controls and patients were treated with 1 μM dG and/or 1 μM forodesine for 5 days. For inhibition of GUK1 activity, we treated control cells with 1 μM of P1-(5′-adenosyl) P5-(5′-guanosyl) pentaphosphate (Ap5G; Jena Bioscience) dissolved in sterile phosphate buffer solution (PBS) prior to addition to culture medium for 5 days. The cells were collected and analyzed after treatments. For overexpression of GUK1 isoforms, patients' and controls' fibroblasts were electroporated with the commercial myc-DDK tagged, pCMV6-Entry plasmids GUK1 218aa long isoform (NM_001159390), GUK1 197aa isoform short isoform (NM_001242839), and pCMV6-Entry empty vector (Origene), using the Amaxa Nucleofector II (Lonza) and Amaxa NHDF nucleofector kits (Lonza, #VPD-1001). After electroporation, the cells were transferred to culture medium and plated in 6-well plates. Five days after nucleofection, the cells were collected for the analyses.

Muscle Histopathology

Muscle biopsies were obtained from quadriceps, during routine clinical diagnostic evaluations of the patients. Tissues were fixed in formalin, or unfixed and immediately frozen in isopentane-liquid nitrogen. Hematoxylin and eosin (H&E), succinate dehydrogenase (SDH), and cytochrome c oxidase (COX) staining were performed as previously described.[23]

mtDNA Quantitation

Copy number of mtDNA was assessed by real-time polymerase chain reaction (PCR) using a QuantStudio 3 Real-Time PCR system (Applied Biosystem) with TaqMan MGB probes. Multiplex quantitative PCR in muscle biopsies, blood cells, and fibroblasts were performed for both mtDNA and nDNA using 12S rRNA (Thermo Fisher) and RNase P probes (Applied Biosystems). The relative proportion of mtDNA to nDNA in probands was compared with controls tested at the same time.

Gene Expression Analyses

RNA from skin fibroblasts was extracted using Real NucleoSpin RNA Mini kit for RNA purification (MACHEREY-NAGEL). Total RNA was used to generate cDNA. GUK1 transcripts A and B share 7 exons; however, transcript A contains an additional initial exon, which encodes the mitochondrial targeting sequence (Supplementary Fig S1). To measure the total levels of transcripts A and B, we have used a pair of primers against a shared exon (primer pair 1 that amplifies a segment of exon 5 in transcript A and exon 4 in transcript B). To assess the level of only transcript A, we have used a pair of primers that amplifies an only segment of exon 1 of transcript A (primers pair 2). To determine the level of transcript B, we have subtracted the amount of transcript A from the total transcript. Amplification of human GUK1 isoforms and β-ACTIN as a loading control was performed using iTaq Universal SYBR Green Supermix (Bio-Rad) and quantitative real-time PCR using a QuantStudio 3 Real-Time PCR system (Applied Biosystem).

Western Blot Analysis of Whole Cell Extracts and Mitochondrial Fractions

Western blot and mitochondria isolation were processed as previously described.[24,25] Band quantification was carried out using a c300 Image Station (Azure Biosystems) and ImageJ software (National Institutes of Health [NIH]). The following primary antibodies were used: anti-GUK1 (Abcam), anti-DDK (Origene), anti-vinculin (Abcam), anti-β-actin (Sigma), and anti-VDAC1 (Abcam).

Immunofluorescence

Fibroblasts were grown in 35-mm glass-bottom dishes (MatTek Corporation, P35G-1.5–14-C). Forty-eight hours after transfection, the cells were stained for 30 minutes with 100 nM MitoTracker DeepRed FM (Thermo Fisher Scientific) at 37°C. The immunofluorescence assay was performed as previously described.[26] Primary antibodies (DKK, Origene, and Tomm20; Abcam) fluorescence-labeled secondary Alexa Fluor 594 or

488 (Invitrogen), and DAPI for nuclear staining were used.

GUK1 Activity

GUK1 activity was assessed by incubating total cell extracts in the presence of excessive GMP and ATP and measuring the amount of GDP + GTP formed. Under these conditions, GUK1 catalyzes the phosphorylation of GMP to GDP and the nucleoside diphosphate kinases, further phosphorylates the formed GDP to GTP.

For total GUK activity in fibroblasts, a confluent 152 cm^2 culture dish was pelleted and the cells lysed using a 30-gauge needle. The pellets were discarded, and protein concentrations in the supernatants (total cell extract) were determined.

For the measurement of GUK activity, 20 μg of protein was from each total extract was used. GDP and GTP were quantified using liquid chromatography coupled to tandem mass spectrometry (LC–MS/MS), as previously described.[27]

dNTPs Measurement

Mitochondrial dNTPs were extracted by acidic precipitation, as previously described.[24]

Mitochondrial dNTPs were quantified following a primer extension assay using a previously designed short common primer oligonucleotide annealed to a longer-hanging template oligonucleotide.[28]

Statistical Analysis

Statistical analyses were performed using Prism 9 scientific software. Data are expressed as the mean ± SD of 3 to 16 replicates per group. The experimental groups were evaluated against controls using the Mann–Whitney (nonparametric) test. A p value of < 0.05 was considered to be statistically significant. For analysis of skeletal muscle variant allele frequencies, skeletal muscle whole exome sequencing (WES) data were processed and summarized into percents of variants below cutoffs for allele frequencies ranging from 0 to 1 at 0.001 intervals. We then summarized individual sample level whole exon sequence data using areas under the curve and compared the areas between probands and controls using the 2-sample t test.

Results

Clinical Presentations

Proband 1 is a 33-year-old man who was born to healthy non-consanguineous parents with a low birthweight of 5.3 pounds (first percentile; Table). Evaluation at age 10 months, revealed low weight (10th percentile), cutaneous telangiectasia, hepatomegaly, and elevated serum transaminases. After discontinuing nursing and beginning cow's milk, both weight and liver abnormalities improved. At age 11 years old, abdominal pain prompted a computed tomography (CT) scan that revealed hepatomegaly. Liver transaminases (aspartate transaminase [AST] 81 U/L [normal 5–40] and alanine transaminase [ALT] 211 U/L [normal 5–40]) and triglycerides (212 mg/dL [normal 60–135]) were elevated. Liver biopsy revealed hepatic

TABLE. Clinical, Histological, and Molecular Genetic Characteristics of Patients With *GUK1* Pathogenic Variant [Color table can be viewed at www.annalsofneurology.org]

Proband	Sex	Current age	Age of onset	First manifestation	Skeletal muscle: Ptosis	Ophthalmoparesis	Chronic fatigue	Elevated creatine kinase	Limb muscle atrophy	Limb muscle weakness	Scoliosis	Muscle biopsy: Ragged-red fibers	COX-negative fibers	Myofiber size variation	Mild focal fibrosis Endomysium	mtDNA Depletion	mtDNA Deletions	Mitochondrial respiratory chain deficiencies	Heart: Cardiomyopathy	Nervous system: Brain MRI white matter T2-hyperintensity	Migraine headaches	Severe depression	Chronic anxiety	Chronic insomnia	Autism spectrum disorder	Hearing loss	Peripheral neuropathy	Areflexia	Liver: Hepatomegaly	Elevated transaminases	Elevated triglycerides	Immune system: Frequent infections	Reduced CD4 lymphocytes	Skin: Skin telangiectasias	GI system: Gastrointestinal dysmotility	Endocrine: Glucose intolerance	Other: Enlarged parotid glands
1	M	33	0	Hepatomegaly	+	+	+	+	+	+	+	+	+	+	+	+	+	+	+	–	+	+	+	–	–	+	+	+	+	+	+	+	+	+	–	+	+
2	F	31	0	Failure to thrive	+	–	+	+	+	–	+	+	+	+	–	+	+	–	+	+	+	–	–	–	–	–	+	–	+	+	+	+	+	–	–	–	–
3	F	37	6	Ptosis	+	–	+	+	+	–	+	+	+	+	–	+	+	–	–	–	–	–	–	–	–	–	–	–	–	+	–	–	+	+	–	–	–
4	F	34	16	Ptosis	+	+	+	–	+	–	+	+	+	+	–	+	+	–	–	–	–	–	–	–	–	–	–	–	–	+	–	–	–	–	–	–	–

GI = gastrointestinal; MRI = magnetic resonance imaging.

steatosis. In addition, his arms and legs were notably thin relative to his face and trunk.

At age 15 years, a psychiatrist diagnosed him with autism spectrum disorder. Although he performed well on academic testing, he was unable to attend school full-time due to chronic insomnia and fatigue. In addition to prominent muscle atrophy and weakness in the proximal arms and legs, he had kyphoscoliosis and parotid swelling. Laboratory tests revealed elevations of venous lactate (3.3 mM [normal 0.5–2.2]) and creatine kinase (CK; 8,383 U/L [normal 35–230]). The following year, he developed recurrent infections, heat intolerance, difficulty urinating, ptosis, ophthalmoparesis, dysphagia, and decreased tendon reflexes. Immunological evaluation revealed a low CD4 T lymphocyte count (251 cells/mm^3; [normal 300–1,400]) with normal absolute lymphocyte, CD8, B-cell, and natural killer cell counts, resulting in a low CD4 to CD8 T-cell ratio (0.62 [normal 1.0–3.6]), indicating an immunodeficiency, consistent with his history of recurrent infections.

Muscle biopsy showed 20% ragged-red fibers by modified Gomori trichrome stain and ~25% COX-deficient fibers with mildly increased central nuclei, indicating mitochondrial myopathy (Fig 1A). Electron microscopy identified excessive and structurally abnormal mitochondria with paracrystalline inclusions, abnormal cristae, and large electron dense bodies in the matrix. Biochemical tests of skeletal muscle, revealed low activities of mitochondrial complexes I, I + III, II + III, and III, with elevated activities of complex II and citrate synthase (Supplementary Table S1). Muscle mtDNA depletion (18% relative to control muscle) but no deletions were detected. Depletion of mtDNA was also detected in blood monocytes, neutrophils, lymphocytes, and platelets (Fig 1C) and primary skin fibroblasts (55% relative to control fibroblasts; see Fig 1C).

Proband 2, the 31-year-old sister of proband 1, had a low birthweight of 4.7 pounds (first percentile) and had frequent infections through childhood and adolescence. During early childhood, she developed migraine headaches, proximal limb weakness, and heat and exercise intolerance, as well as elevated serum CK and transaminases (see Table). By age 11 years, depression and tremors developed. At age 16 years, triglycerides (166 mg/dl), AST (75–127 U/L), ALT (41–114 U/L), and CK (767–1,344 U/L) were elevated. Clinical examination and liver ultrasound were normal. Blood studies revealed low to normal white cell counts (2,920–4,920/mm^3 [normal 4,300–10,000]) with low total lymphocytes (950–980 cells/mm^3 [normal 1,000–4,800]), low CD4 T lymphocyte count (129–178 cells/mm^3) with normal CD8, B-cell, and natural killer cell counts, with low CD4 to

CD8 T-cell ratios (0.31–0.53). By age 19 years, she developed chronic dull headaches with occasional severe sharp stabbing pains and episodes of mental fogginess that lasted up to 4 days. Magnetic resonance imaging (MRI) revealed a single punctate focus of fluid attenuated inversion recovery (FLAIR) hyperintensity in the left parietal white matter. Brain magnetic resonance (MR) spectroscopy did not identify a lactate peak. She also developed mild ptosis and stocking sensory loss with decreased cold, vibration, and sharp sensations. In contrast to her brother, proband 1, she has not developed ophthalmoparesis, limb muscle atrophy, kyphoscoliosis, glucose intolerance, parotid swelling, autistic spectrum disorder, or skin telangiectasia.

At age 17 years, a muscle biopsy revealed striking variation in fiber size, increased central nuclei, scattered necrotic fibers, ragged-red fibers, and numerous COX-negative fibers, indicating mitochondrial myopathy. Electron microscopy identified muscle fibers with coarse granular material and malformed mitochondria, including mitochondria devoid of central cristae. Muscle respiratory chain enzyme activities of complexes III, IV, CI + III, and CII + III were low, and CII and CS were elevated (see Supplementary Table S1). The muscles also showed mtDNA depletion (52% relative to the control muscle) but no deletions. Depletion of mtDNA was also observed in blood monocytes, neutrophils, and lymphocytes, and cultured skin fibroblasts (55% relative to control fibroblasts; see Fig 1B, C).

Proband 3 is a 37-year-old woman who had bilateral palpebral ptosis at age 6 years (see Table). At age 30 years, she developed distal and proximal muscle weakness, with mildly elevated serum CK (278 U/L). A muscle biopsy revealed ragged-red fibers and increased muscle fiber size variability. Muscle respiratory chain enzyme activities showed decreases of all complexes except for complex II and citrate synthase (see Supplementary Table S1). Although the skeletal muscle mtDNA quantity was normal, multiple mtDNA deletions were detected by Southern blot. Blood tests showed elevated lactate dehydrogenase (LDH; 384 U/L [normal 140–280]), slightly elevated transaminases (AST = 50 U/L, ALT = 41 U/L, and gamma-glutamyl transferase [GGT] = 56 U/L [normal 5–40]), and reduced CD4 (146 cells/mm^3) and CD8 (210 cells/mm^3) lymphocytes, resulting in a low CD4 to CD8 T-cell ratio (0.70). Blood lymphocytes, monocytes, and neutrophils showed reduced mtDNA levels (60% relative to control fibroblasts) that was also apparent in skin fibroblasts (see Fig 1B, C). Lungs showed moderate obstructive disorder and bronchial hyperactivity attributed to bronchial asthma diagnosed during infancy.
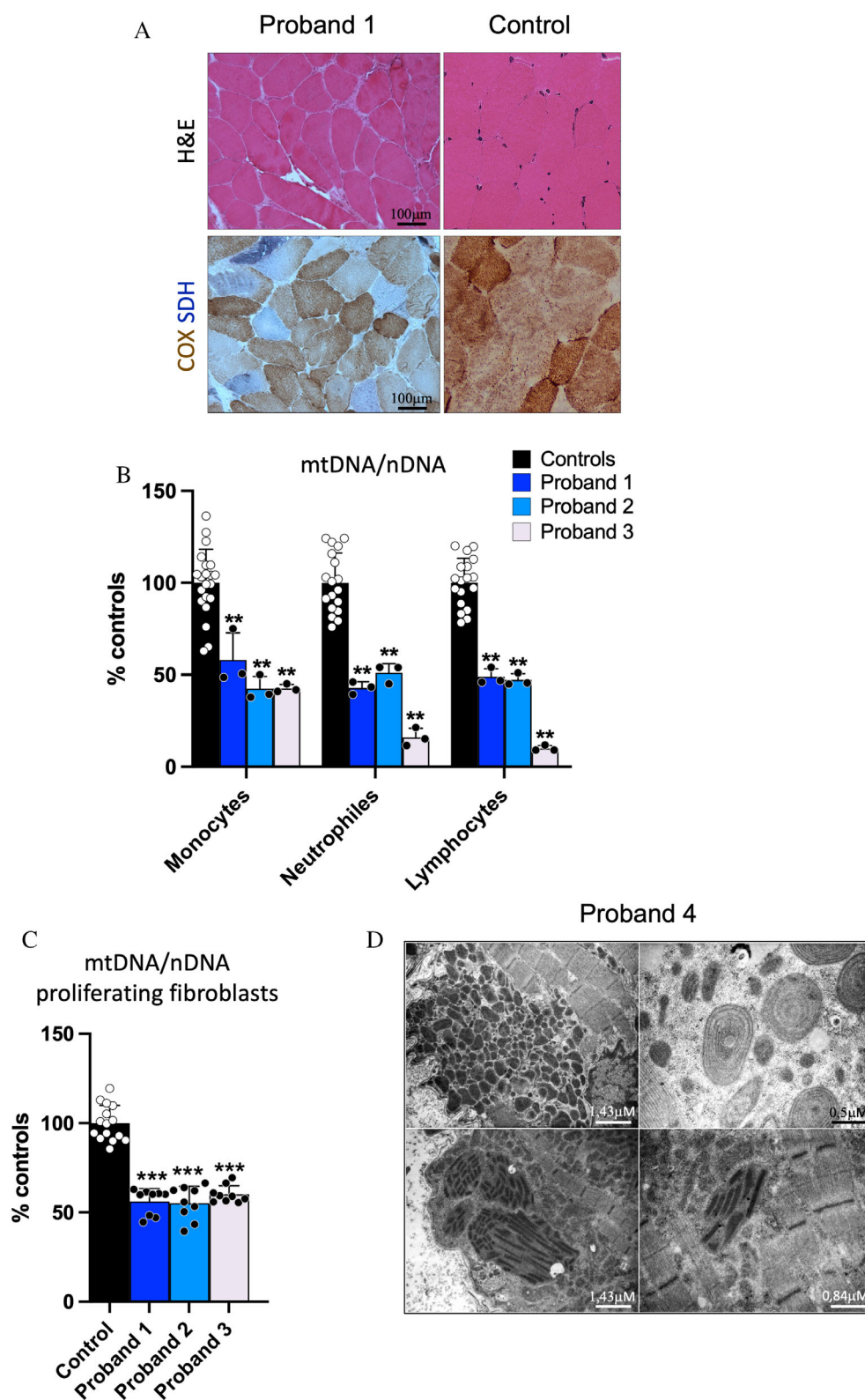
FIGURE 1: Histological and molecular genetic features of GUK1 deficient probands. (A) Cross sectional skeletal muscle biopsy histochemically stained with hematoxylin and eosin (H&E), cytochrome C oxidase (COX), and succinate dehydrogenase (SDH) from proband 1 and controls. **(B)** Percentages of mtDNA levels of probands' 1, 2, and 3 monocytes, neutrophiles, lymphocytes and platelets relative to controls. **(C)** Percentages of mtDNA levels of probands' 1, 2 and 3 fibroblasts relative to controls. **(D)** Electron microscopy of skeletal muscle biopsy of proband 4, showing altered mitochondrial morphology. Data are expressed as mean ± standard deviation (SD). *$p < 0.05$, **$p < 0.01$, ***$p < 0.001$ differences versus controls fibroblasts (Mann–Whitney test; 3–5 controls fibroblast were used and $n = 3–4$ for each group). [Color figure can be viewed at www.annalsofneurology.org]

Proband 4, is a 34-year-old woman who was born to healthy non-consanguineous parents with no relevant family history of neuromuscular disorders. At age 16 years, she developed progressive bilateral ptosis and chronic muscle fatigue. At 19 years old, she underwent a muscle biopsy that revealed ragged-red fibers and several COX-negative/succinate dehydrogenase (SDH)-positive fibers. Electron microscopy showed collections of mitochondria with abnormal shapes and dimensions as well as altered cristae organization and distribution. Enlarged mitochondria contained paracrystalline inclusions of heterogeneous size (Fig 1D).

An examination at age 34 years revealed normal mental status, bilateral ophthalmoplegia and ptosis, a high arched palate, areflexia of the legs, and proximal limb weakness. Brain MRI and cardiac evaluations were normal. Electromyography showed both chronic neurogenic and myopathic abnormalities. She did not have headaches, hearing loss, seizures, stroke-like episodes, or gastrointestinal symptoms.

General laboratory studies were normal except for elevated serum CK (728 U/L) and lactate (4.05 mmol/L) levels. Immunological screening did not indicate immunodeficiency or low CD4 count.

Whole mtDNA sequencing of skeletal muscle revealed no pathogenic variants. Southern blot analysis of skeletal muscle detected multiple mtDNA deletions and depletion, confirmed by qPCR analysis (22% relative to controls). Biochemical tests revealed defects in the activities of mitochondrial complex I, I + III, II + III, and IV and increased activity of citrate synthase in skeletal muscle (see Supplementary Table S1).

Characterization of GUK1 Variants

We identified 5 GUK1 variants in 3 unrelated families; 3 affect both isoforms (isoform A and B) and 2 affect only isoform A (Fig 2A–E).

Whole exome sequencing (WES) of probands 1 and 2 revealed biallelic GUK1 variants. Sanger DNA sequencing of the probands and their parents confirmed inheritance of each pathogenic variant from the healthy heterozygous parents (see Fig 2A, B). A paternal GUK1 c.66_67insGCTGCGGCGCCCGCTGGCCGGGCTG in NM_001159390 (transcript A) and c.3_4insGCTGCGGC-GCCCGCTGGCCGGGCTG in NM_001242839 (transcript B) causing frameshifts, truncating both GUK1 isoforms (NP_001152862 and NP_001229768; see Fig 2B). The maternal GUK1 variant, c.94G>A (transcript A) and c.31G>A (transcript B), results in a p.Gly32Arg amino acid substitution in GUK1 isoform A and p.Gly11Arg missense GUK1 isoform B. GUK1 Gly32

(isoform A)/Gly11(isoform B) is highly conserved (see Fig 2C) and Arg32(isoform A)/Arg11(isoform B) is predicted to be deleterious by PROVEAN variant prediction software (PROVEAN score = −7.41, [cutoff −2.5]) and pathogenic by AlphaMissense (score 0.985 [cutoff 0.564]; DeepMind Technologies Limited).[29,30] Gly32/Gly11 is an essential component of the GUK1 P-loop, which binds ATP to facilitate phosphate transfer to (d)GMP (see Fig 2C).

In proband 3, WES revealed a homozygous GUK1 variant c.61 + 1G>T (transcript A) predicted to alter only isoform A (see Fig 2D). This variant modifies a canonical splice donor sequence and produces an aberrant splicing that incorporates 4 intronic nucleotides into GUK1 transcript A, resulting in a frameshift that leads to a premature termination codon (p.Gly21ValfsTer65). Both parents and daughter of proband 3 were heterozygous for the variant.

In Proband 4, WES revealed a GUK1 paternally inherited heterozygous variant affecting both isoforms c.139C>T (transcript A) and c.76C>T (transcript B). This variant is predicted to generate a premature termination codon in both GUK1 isoforms (p.Gln47* in isoform A and p.Gln26* in isoform B; see Fig 2E). Sanger resequencing of a WES low-coverage region encompassing GUK1 exon 1 revealed a maternally inherited heterozygous start codon substitution c.2 T>G (transcript A, p.Leu2_Met22del) affecting only the isoform A (see Fig 2E).

Assessment of GUK1 Splice Variants

To assess isoform expression and potential functional differences of the GUK1 splice variants, we analyzed the relative abundance of GUK1 transcripts and protein expression levels in available fibroblasts from probands 1 to 3. The fibroblasts from probands 1 and 2 exhibited decreased total GUK1 mRNA levels, with proband 1 showing a 54% and proband 2 showing a 75% total GUK1 mRNA relative to controls (Fig 2F). Both probands showed similar transcripts proportions (24% transcript A and 76% transcript B) compared with controls (30% transcript A and 70% transcript B; Fig 2G). In proband 3 fibroblasts, total GUK1 mRNA levels were severely decreased (28% relative to controls; see Fig 2F), consisting entirely of transcript B suggesting nonsense-mediated mRNA decay of the longer transcript (see Fig 2G).

Western blot analyses of GUK1 proteins in fibroblasts of probands 1 and 2 revealed reductions in isoform B (21.7 kDa) and undetectable isoform A (23.8 kDa; Fig 3A), whereas proband 3 fibroblasts showed similar GUK1 levels compared with controls.
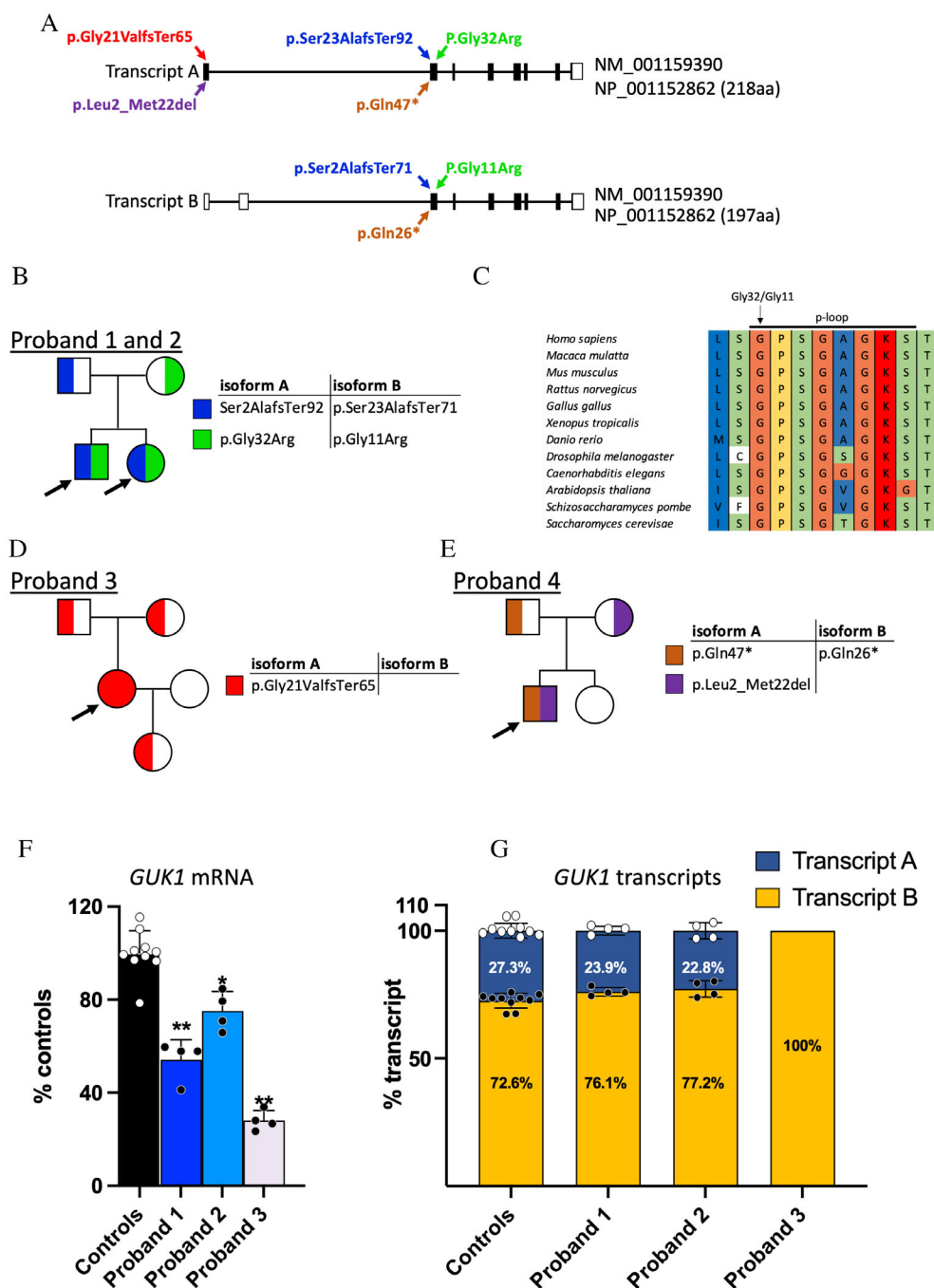
FIGURE 2: *GUK1* pathogenic variants in the four probands. (A) Schematic representation of the 2 major GUK1 transcripts. (B) Pedigree of proband 1 and 2 and *GUK1* variants. (C) Evolutionary conservation of GUK1 p.Gly32 (isoform A)/Gly11 (isoform B) and p-loop segment across species. (D) Pedigree of proband 3 and *GUK1* variant. (E) Pedigree of proband 4 and the pathogenic variants. (F) Percentage of the total GUK1 mRNA level in fibroblasts of probands 1, 2, and 3 relative to control fibroblasts. (G) Proportions of *GUK1* transcripts A and B in control and probands' 1, 2, and 3 fibroblasts. Data are expressed as mean ± SD. *$p < 0.05$, **$p < 0.01$ differences versus controls fibroblasts (Mann–Whitney test; 3–4 controls fibroblast were used and $n = 4$ for each group). [Color figure can be viewed at www.annalsofneurology.org]

GUK1 Subcellular Localization

To further examine differences between the GUK1 isoforms, given the divergent effects of the pathogenic variants in the patients, we evaluated GUK1 subcellular localization. According to The Human Protein Atlas (proteinatlas.org), UniProt (UniProt.org), and published studies, GUK1 is a cytosolic protein.[15] However, GUK1 is listed as a mitochondrial protein in MitoCarta and in the MitoCop databases.[31,32] Three mitochondrial targeting peptide prediction programs (TargetP-2.0,

MitoFates, and iPSORT), indicated that isoform A, but not isoform B, contains a mitochondrial targeting sequence. Western blot using whole-cell extracts and mitochondria isolated from control fibroblasts demonstrated that the mitochondrial fraction contained isoform A but not isoform B, although both isoforms were detected in whole cell extracts (Fig 3B). In contrast to controls and consistent with findings in whole cell extract, isoform A was not detected in probands' mitochondria (see Fig 3A).

To confirm the mitochondrial localization of isoform A, we separately overexpressed isoforms A and B and empty vector (EV) in proband fibroblasts. As expected, we observed both nucleofected GUK1 isoforms A and B (with higher molecular weights than their natural isoforms due to Myc-DDK tags in the C-terminus: 27.4 kDa for isoform A and 25.3 kDa for isoform B) in whole cell extracts (Fig 3C and Supplementary Fig S2B). In mitochondrial fractions, we identified only nucleofected isoform A using both anti-DDK (Flag) and anti-GUK1 antibodies (Fig 3D). By immunofluorescence, we confirmed mitochondrial localization of only nucleofected isoform A using an anti-DDK antibody co-immunostained with MitoTracker dye or anti-TOM20 antibody (Fig 3E, and Supplementary Fig S2A).

GUK1 Deficiency Causes mtDNA Depletion

To confirm that decreased GUK1 activity causes mtDNA depletion, we treated control fibroblasts with P1-(5′-adenosyl) P5-(5′-guanosyl) pentaphosphate (AP$_5$G), a GUK1 inhibitor[16,33] and confirmed reduced mtDNA content (52% relative to vehicle; Fig 4A). We then demonstrated functions effects of the probands' GUK1 variants by detecting decreased GUK1 activity in all 3 available probands' fibroblasts compared with healthy controls (Fig 4B). Transient expression of GUK1 isoform B increased mtDNA levels in controls fibroblasts, indicating potential involvement of cytosolic GUK1 in mtDNA maintenance in normal replicating cells (Fig 4C). We observed partial increase of mtDNA by expressing isoform B (low efficiency plasmid) at levels similar to controls cells (see Fig 4E and Supplementary Fig S3A). We demonstrated complete recovery of mtDNA levels in probands' 1 to 3 fibroblasts after nucleofection with isoform A and no changes after nucleofection with EV (see Fig 4D, E), suggesting that although both isoforms are important for mtDNA maintenance, isoform A may be more critical than isoform B. We noted 30 to 40 fold greater expression of isoform A than B (see Supplementary Fig S3B), when we overexpressed isoform B (high efficiency plasmid) to the same level as isoform A (see Supplementary Fig S3B),

with the low efficiency plasmid (see Supplementary Fig S2B, C, and Supplementary Fig S3C), further indicating that isoform A is more critical than B to maintain mtDNA in mitotic cells. We also observed mtDNA depletion in all 3 proband fibroblasts in quiescence demonstrating importance of the mitochondrial deoxyguanosine salvage pathway in maintaining mtDNA in post-mitotic cells (Fig 4F).

Given the function of GUK1 and previous reports implicating unbalanced dNTP pools in other forms of MDDS,[6–13] we measured dNTP concentrations in proliferating proband fibroblasts and observed expected reduced dGTP (52–75% relative to control), but increased dTTP (152–165% relative to control) levels (Fig 4G).

Measurements of mitochondrial complexes I + III, IV, and citrate synthase in fibroblasts showed no deficits in probands cells compared with the controls indicating that the partial in vitro mtDNA depletion was insufficient to cause bioenergetic defects (Supplementary Fig S4).

Nucleoside Supplementation and Maintenance Rescues mtDNA Depletion

Due to the role of GUK1 in dGTP synthesis and observed dGTP reduction in proband fibroblasts, we assessed whether dGTP augmentation would rescue the mtDNA depletion in vitro. Because exogenous nucleotides are incorporated by cells,[27,34,35] we hypothesized that increasing deoxyguanosine (dG) by supplementing cell media with excess of dG or inhibiting purine nucleoside phosphorylase (PNP) could enhance deficient GUK1 activity and increase levels of dGTP. PNP is a key enzyme in the purine salvage pathway, and its inherited deficiency leads to accumulation of dGTP by preventing the recycling of purines.[36] After 5 days of supplementation of media with 1 μM of dG or 1 μM of the PNP inhibitor, forodesine, alone (Fig 5A) or in combination (Fig 5B), mtDNA content in probands' fibroblasts increased to control fibroblast levels.

No Significant Impact of GUK1 on nDNA

As described above, GUK1 is involved in both de novo and salvage nucleotide synthesis pathways. Therefore, to assess whether GUK1 deficiency impacts nDNA, we assessed WES data to search for potential alterations of variant allele frequencies (VAFs) in available fibroblasts and skeletal muscle biopsies from the probands and controls. In fibroblasts, areas under curves for percents of variants across allele frequencies indicates no significant changes (p value = 0.65; Fig 6A). In the case of skeletal muscle, a trend toward higher percentages of variants in skeletal muscles of 3 probands compared with 3 controls (p value = 0.07) where found (Fig 6B). However, we did
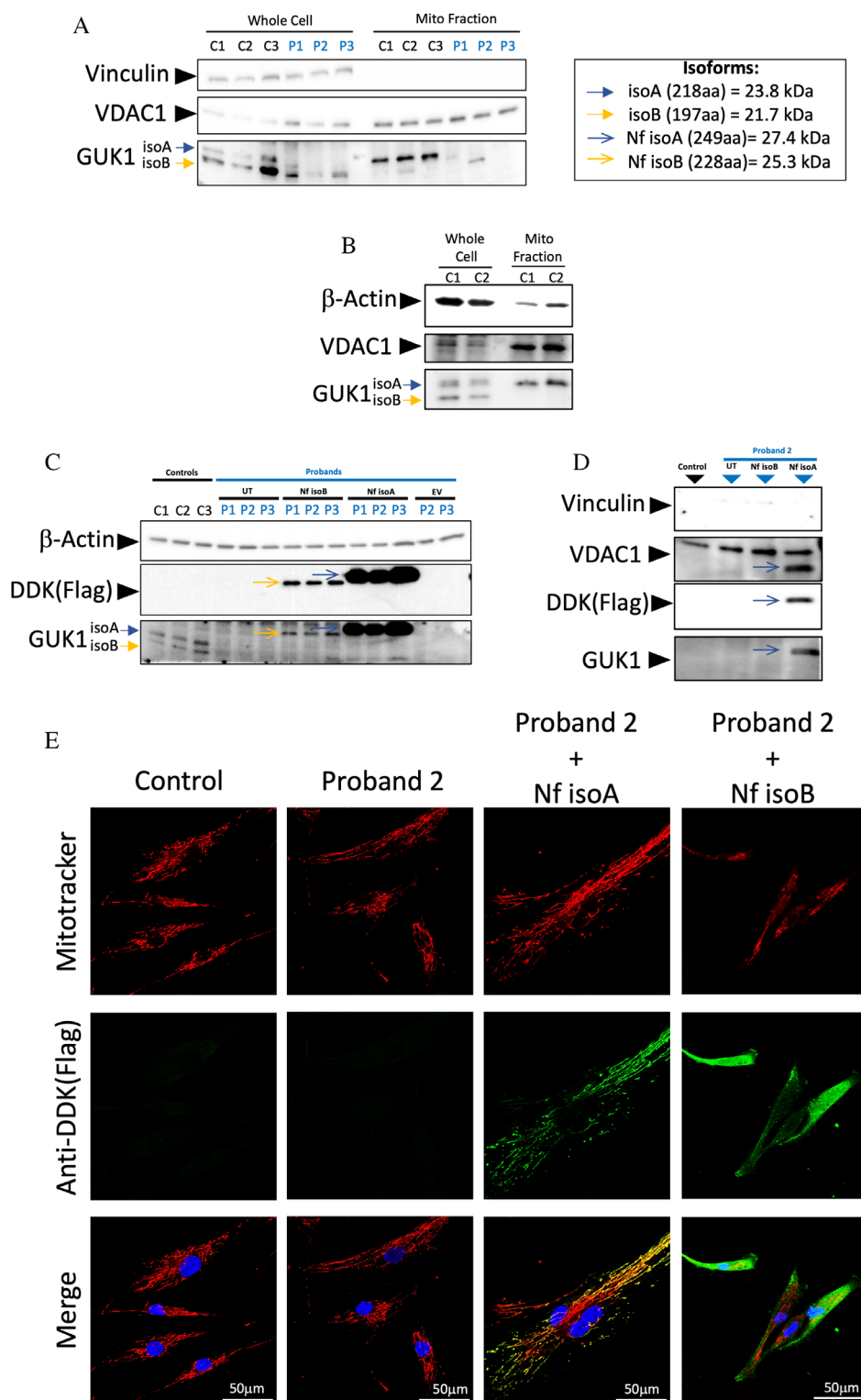
FIGURE 3: Mitochondrial localization of 218aa long GUK1 isoform. (A) Representative Western blotting of GUK1 isoform A (isoA) and isoform B (isoB) in whole cell extract and mitochondrial fractions of control and probands' 1, 2, and 3 fibroblasts. (B) Representative Western blots of GUK1 isoA and isoB comparing whole cell extract against mitochondrial fraction in controls fibroblasts. (C) Western blots of GUK1 in whole cell extract of control fibroblasts; untransfected (UT) fibroblasts of probands' 1, 2 and 3; fibroblasts of 1, 2 and 3 probands nulceofected with isoform A (Nf isoA); probands 1, 2, and 3 fibroblasts nucleofected with isoform B (Nf isoB) and probands' 1, 2, and 3 fibroblasts nucleofected with empty vector (EV). (D) Western blots of GUK1 using mitochondrial fraction of control fibroblasts, untransfected proband 2 fibroblasts, Nf isoA proband 2 fibroblasts, and Nf isoB proband 2 fibroblasts. (E) Immunofluorescence of DDK (Flag) and Mitotracker to stain the mitochondria in control fibroblasts, untransfected proband 2 fibroblasts, Nf isoA proband 2 fibroblasts, and Nf isoB proband 2 fibroblasts. [Color figure can be viewed at www.annalsofneurology.org]
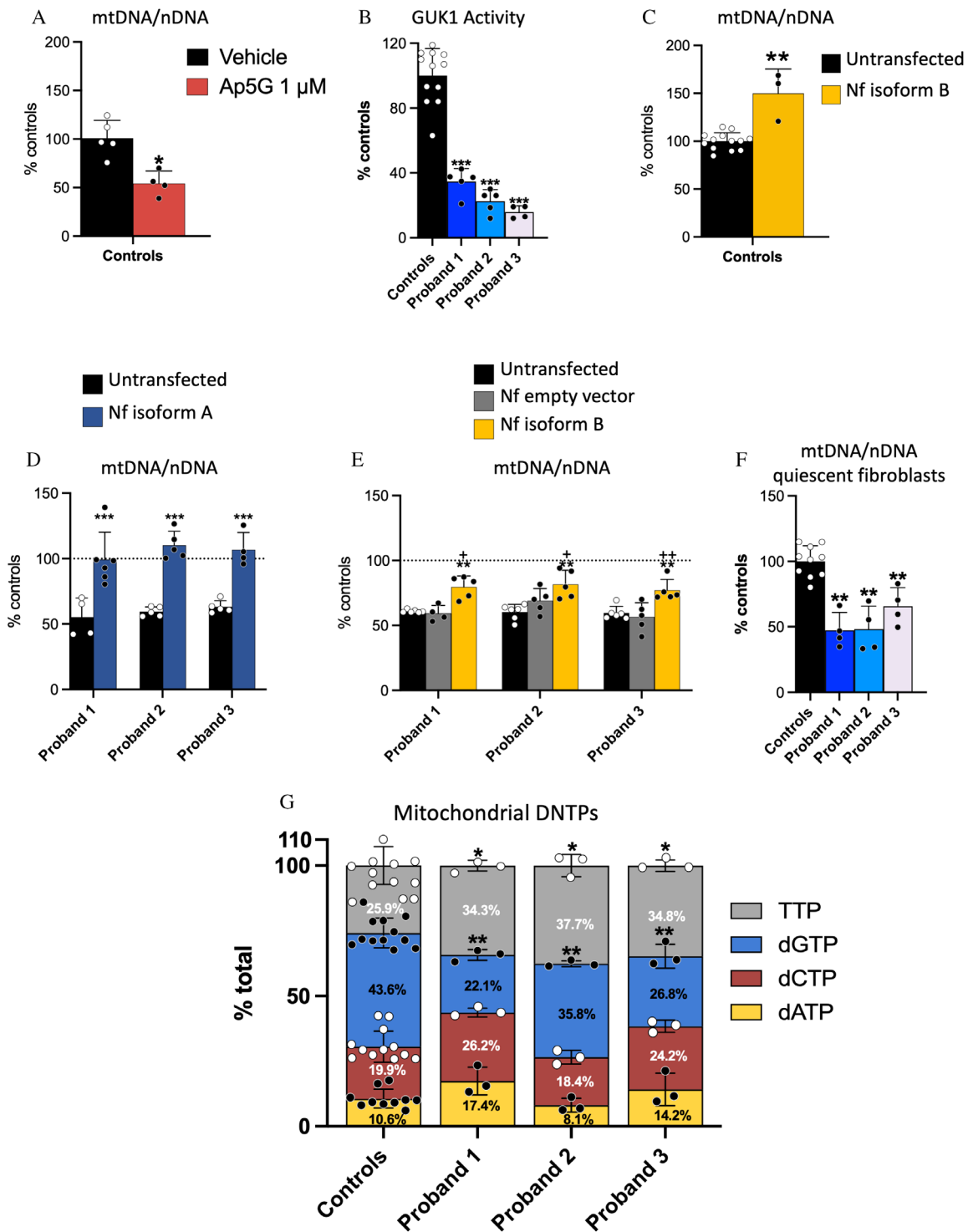
FIGURE 4: Functional assessments of GUK1 variants and pharmacological inhibition. (A) Percentage of the mtDNA levels of control fibroblasts and control fibroblasts after treatment with 1 mM of GUK inhibitor Ap5G relative to controls. (B) GUK1 activity in control and probands' 1, 2, and 3 fibroblasts. (C) Percentage of the mtDNA levels in control fibroblasts and control Nf isoB relative to control fibroblasts. (D) Percentage of the mtDNA levels of untransfected probands' 1, 2, and 3 fibroblasts and Nf isoA probands' 1, 2, and 3 fibroblasts relative to control fibroblasts. (E) Percentage of the mtDNA levels of untransfected probands' 1, 2, and 3 fibroblasts, Nf isoB probands' 1, 2, and 3 fibroblasts and Nf empty vector probands' 1, 2, and 3 fibroblasts relative to control fibroblasts. (F) Percentage of the mtDNA levels of probands' 1, 2, and 3 fibroblasts in quiescent conditions relative to control fibroblasts. (G) Mitochondrial dNTPs pool percentages in probands' 1, 2, and 3 fibroblasts relative to control fibroblasts. Data are expressed as mean $\pm$ SD. *$p < 0.05$, **$p < 0.01$, ***$p < 0.001$ differences versus controls. $^{+}p < 0.05$, $^{++}p < 0.01$ Transfected with 197aa isoform versus transfected with empty vector (Mann–Whitney test; 3–4 controls fibroblast were used and $n = 3$–5 for each group). [Color figure can be viewed at www.annalsofneurology.org]
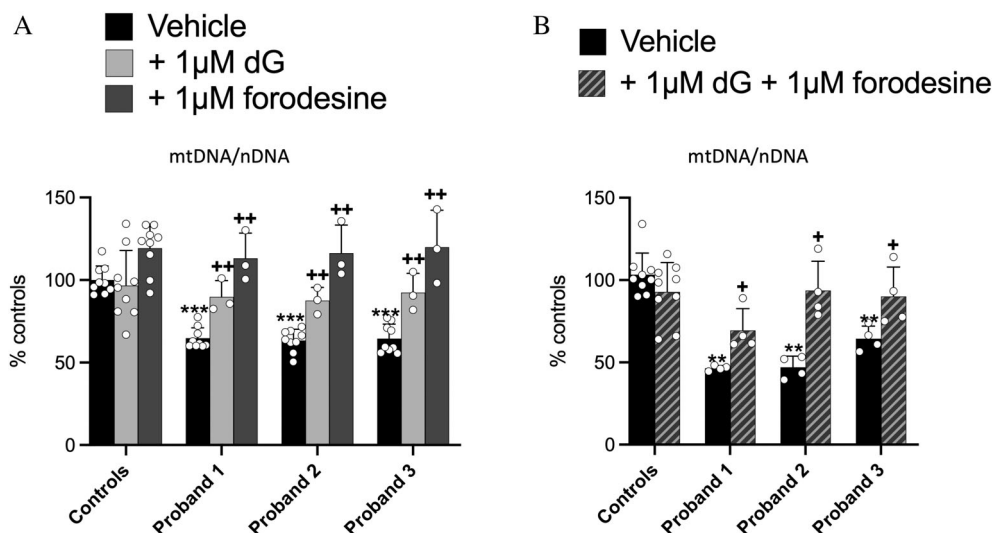
FIGURE 5: In vitro pharmacological treatment of GUK1 deficiency. (A) Percentages of the mtDNA levels of control and probands' 1, 2, and 3 fibroblasts after treatment with vehicle, 1 mM of dG, or 1 mM forodesine, relative to control fibroblasts. (B) Percentages of the mtDNA levels of control and probands' 1, 2, and 3 fibroblasts after treatment with vehicle or a combination of 1 mM dG + 1 mM forodesine, relative to control fibroblasts. Data are expressed as mean ± SD. *$p < 0.05$, **$p < 0.01$, ***$p < 0.001$ differences versus controls. +$p < 0.05$, ++$p < 0.01$ untreated fibroblasts versus treated fibroblasts (Mann–Whitney test; 3–4 controls fibroblast were used and $n = 3$–4 for each group).

not observe a functional effect on nDNA replication based upon similar proliferation rates of fibroblasts from probands and controls (Fig 6C).

Discussion

Our studies demonstrate that *GUK1* pathogenic variants constitute a novel genetic cause of MDDS. The identified variants led to reduced guanylate kinase activity and dNTP pool imbalance, which causes MDDS.

An unusual clinical feature of GUK1 deficiency compared to other MDDS disorder is the prominent immunological abnormalities with decreased T lymphocyte counts. One potential explanation is that, unlike other causative genes for mtDNA depletion/deletion syndrome (MDDS), *GUK1* has 2 isoforms: one mitochondrial and the other cytosolic. Thus, deficiency of the mitochondrial isoform is responsible for mtDNA depletion and deletions, whereas the defective cytosolic form may alter cellular purine nucleotide pools that preferentially damage T cells. In fact, genetic disorders of purine metabolism, such as adenosine deaminase deficiency and purine nucleoside phosphorylase deficiency, are well-known causes of immunodeficiency disorders, although the mechanisms by which they occur are not fully characterized.[37]

Including GUK1 deficiency, there are at least 35 monogenic causes of mitochondrial DNA depletion/deletion syndrome (MDDS).[2,11] More than 1,000 patients with MDDS have been identified, but, to our knowledge, there were only 4 patients with MDDS due to GUK1 deficiency; therefore, this new disease accounts for < 0.4% of all MDDS cases. We anticipate that additional patients will be identified with GUK1 deficiency after the first description of this disease is published. Nevertheless, the frequency of this new MDDS disease is expected to remain low.

Although the 4 probands are adults, all had initial manifestations in childhood or adolescence and developed ptosis and skeletal myopathy. Probands 1 to 3 also developed hepatopathy, and lymphocytopenia with low T4 cell counts. Probands 1 and 2 had additional manifestations, including encephalopathy, peripheral neuropathy with reduced tendon reflexes, heat intolerance, glucose intolerance, and brain MRI white matter T2 hyperintensities. The differences in clinical features and expression of GUK1 isoforms with mtDNA alterations among the patients and the lack of identified guanylate kinase in mitochondria led us to further investigate the GUK1 isoforms. We have demonstrated that in the mitochondrial fraction of control fibroblasts isoform A is abundant, whereas isoform B was undetectable. In contrast, both isoforms were present in whole cell extracts. In probands 1 and 2, although fibroblasts exhibited reduced total GUK1 mRNA levels and similar proportions of transcripts A and B compared with the controls, we detected GUK1 isoform B protein at reduced levels but not isoform A protein, likely due to very low amounts of transcript A. Regardless of their relative levels, both isoforms express the glycine to arginine missense alteration in the P-loop
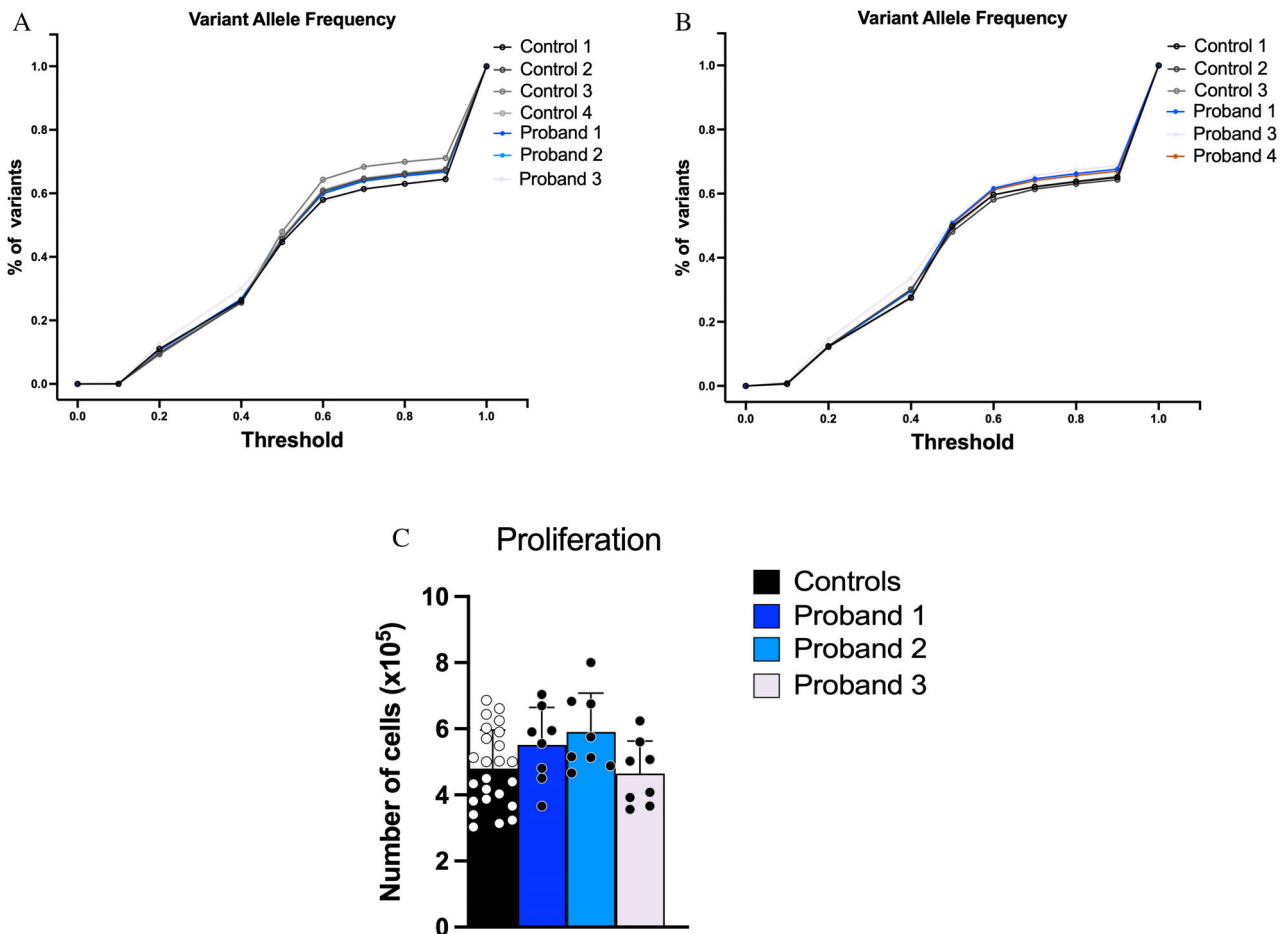
FIGURE 6: No significant effect of GUK1 pathogenic variants on nDNA. (A) Fibroblasts WES data of probands 1, 2, and 3 and 4 healthy controls were processed and summarized into percentages of variants below the cutoffs for allele frequencies ranging from 0 to 1 at 0.001 intervals. Proband skeletal muscle DNA show trends toward higher percentages of variants than the controls over the spectrum of allele frequency thresholds (p value = 0.645). (B) Skeletal muscle WES data of probands 1, 3, and 4 and 3 healthy controls were processed and summarized into percentages of variants below the cutoffs for allele frequencies ranging from 0 to 1 at 0.001 intervals. Proband skeletal muscle DNA show trends toward higher percentages of variants than the controls over the spectrum of allele frequency thresholds (p value = 0.07) (C) Proliferation rates of control and probands' 1, 2, and 3 fibroblasts. [Color figure can be viewed at www.annalsofneurology.org]

that impairs GUK1 activity, which, in turn, leads to dNTP imbalance and mtDNA depletion. In contrast, proband 3 fibroblasts lack GUK1 transcript A due to the isoform-specific pathogenic variant and maintain intact transcript B albeit at only 30% relative to controls. Even in the absence of isoform A, the intact isoform B present in these fibroblasts appears to be able to maintain mtDNA levels around 50%, likely due to the transport of dGDP and/or dGTP to the mitochondria through nucleotide transporters,[19–22] indicating the importance of the cytosolic GUK1 isoform in mtDNA maintenance when isoform A is severely impaired.

To confirm the mitochondrial localization and functional significance of GUK1 isoform A, we performed complementation studies to overexpress both GUK1 isoforms. We identified only GUK1 isoform A in mitochondria and isoform B in cytosol by immunofluorescence and Western blot. Overexpression of either isoform led to mtDNA recovery, supporting the involvement of GUK1 in mtDNA maintenance and confirming that overexpression of the cytosolic isoform can compensate for defects in the mitochondrial isoform in replicating cells; however, mitochondrial isoform A appears to be more important than isoform B in mtDNA maintenance.[19–22]

Having demonstrated the significance of GUK1 in mtDNA maintenance, we investigated whether a defect in this enzyme could impact nDNA. However, consistent with a recent report on MDDS associated with deficiencies in the de novo pathway enzyme RRM1,[11] we did not detect a statistically significant elevation in somatic nuclear variants in fibroblasts. Nevertheless, skeletal muscle of the probands showed trends toward increased frequency of variants that warrant future investigation with a larger

number of samples. There were no discernible changes in cellular proliferation in the fibroblasts of these patients indicating normal rates of nDNA replication.

In addition to identifying *GUK1* variants as a novel genetic cause of MDDS, we have demonstrated that dG supplementation of cultured probands' fibroblasts rescues mtDNA depletion, analogous to reports of *DGUOK* mutant fibroblasts supplemented with dGMP.[38,39] Therapeutic potential of nucleoside supplementation has been demonstrated with pyrimidine nucleoside supplementation of cell and mouse models of TK2 deficiency and compassionate use in patients with TK2 deficiency as well as promising results in cell and animal models for other forms of MDDS.[34,35,40–44] Clinical pyrimidine deoxynucleoside therapy for TK2 deficiency is currently under assessment in a phase II clinical trial,[45,46] whereas dG supplementation may be a viable therapy for GUK1 deficiency.

A barrier to dG supplementation is the rapid catabolism of purines by PNP in vivo.[27] In treating *GUK1* mutant proband fibroblasts, we have applied the PNP inhibitor forodesine to prevent dG degradation and ameliorate mtDNA depletion.[27] Forodesine has been approved for the treatment of individuals with relapsed or refractory peripheral T-cell lymphoma and leukemia in Japan.[47] In support of potential efficacy for *GUK1* deficiency, forodesine administration alone in humans is sufficient to increase dGTP concentrations in peripheral blood.[48] Here, we have confirmed that forodesine alone or in combination with dG increases mtDNA levels in GUK1-deficient probands fibroblasts, suggesting alternative treatment approaches for patients with GUK1 deficiency. Notably, the concentration of forodesine tested is in line with serum concentrations used clinically for treatment of T-cell malignancies.[49] Furthermore, clinical dosing of forodesine elevated plasma dG to levels comparable to those we used in our in vitro studies.[50]

In summary, our findings demonstrate that GUK1 isoform A is the mitochondrial guanylate kinase, GUK1 deficiency is a novel cause of MDDS, and is the first example of impaired NMPK causing MDDS. We have demonstrated successful treatment of GUK1-deficient fibroblasts using dG, forodesine, or their combination to restore mtDNA levels.

Acknowledgments

Author Contributions

A.H.G., J.S., R.M., and M.H. contributed to the conception and design of the study, A.H.G., J.S., J.R., E.B.C., A.P., R.S., G.G., J.C.M., A.M.G., L.G., O.U., Y.G., L.K., T.W., S.T., M.M., M.S., S.W., K.T., M.S.H., M.O.D., M.M., G.P.C., D.R., R.M., A.R., F.T., and M.H. contributed to the acquisition and analysis of data. A.H.G., J.S., S.W., T.W., M.S.H., D.R., R.M., A.R., F.T., and M.H. contributed to drafting the text or preparing the figures.

Potential Conflicts of Interest

M.H. has been a paid consultant to Modis Therapeutics, Inc. (a subsidiary of Zogenix/UCB). This relationship is de minimus for Columbia University Medical Center. M.H. is a co-inventor in Columbia University's patent "Deoxynucleoside Monophosphate Bypass Therapy for Mitochondrial DNA Depletion Syndrome" (US Patent 10,471,087), which has been licensed to Modis Therapeutics; this relationship is monitored by an unconflicted external academic researcher. R.M. has equity in Modis Therapeutics, Inc (a subsidiary of Zogenix/UCB). R.M. is a co-inventor in Columbia University's patent "Deoxynucleoside Monophosphate Bypass Therapy for Mitochondrial DNA Depletion Syndrome" (US Patent 10,471,087), which has been licensed to Modis Therapeutics; this relationship is monitored by an unconflicted external academic researcher. A.H.G., J.S., J.R., E.B.C., A.P., R.S., G.G., J.C.M., A.M.G., L.G., O.U., Y.G., L.K., T.W., S.T., M.M., M.S., S.W., K.T., M.S.H., M.O.D., M.M., G.P.C., D.R., A.R., and F.T. have nothing to report.

Data Availability

All data reported in this paper will be shared by the corresponding author upon request. This work does not use or develop original code. Any additional information required to reanalyze the data reported in this manuscript is available from the corresponding author upon request.

References

1. DiMauro S, Schon EA, Carelli V, Hirano M. The clinical maze of mitochondrial neurology. Nat Rev Neurol 2013;9:429–444.

2. Lopez-Gomez C, Camara Y, Hirano M, et al. 232nd ENMC international workshop: recommendations for treatment of mitochondrial DNA maintenance disorders. 16 – 18 June 2017, Heemskerk, The Netherlands. Neuromuscul Disord 2022;32:609–620.

3. Basel D, Mitochondrial DNA. Depletion syndromes. Clin Perinatol 2020;47:123–141.

4. Hirano M, Pitceathly RDS. Progressive external ophthalmoplegia. Handb Clin Neurol 2023;194:9–21.

5. Carvalho G, Repoles BM, Mendes I, Wanrooij PH. Mitochondrial DNA instability in mammalian cells. Antioxid Redox Signal 2022;36:885–905.

6. Saada A, Shaag A, Mandel H, et al. Mutant mitochondrial thymidine kinase in mitochondrial DNA depletion myopathy. Nat Genet 2001;29:342–344.

7. Mandel H, Szargel R, Labay V, et al. The deoxyguanosine kinase gene is mutated in individuals with depleted hepatocerebral mitochondrial DNA. Nat Genet 2001;29:337–341.

8. Ostergaard E, Christensen E, Kristensen E, et al. Deficiency of the alpha subunit of succinate-coenzyme a ligase causes fatal infantile lactic acidosis with mitochondrial DNA depletion. Am J Hum Genet 2007;81:383–387.

9. Besse A, Wu P, Bruni F, et al. The GABA transaminase, ABAT, is essential for mitochondrial nucleoside metabolism. Cell Metab 2015;21:417–427.

10. Sommerville EW, Dalla Rosa I, Rosenberg MM, et al. Identification of a novel heterozygous guanosine monophosphate reductase (GMPR) variant in a patient with a late-onset disorder of mitochondrial DNA maintenance. Clin Genet 2020;97:276–286.

11. Shintaku J, Pernice WM, Eyaid W, et al. RRM1 variants cause a mitochondrial DNA maintenance disorder via impaired de novo nucleotide synthesis. J Clin Invest 2022;132:e145660.

12. Bourdon A, Minai L, Serre V, et al. Mutation of RRM2B, encoding p53-controlled ribonucleotide reductase (p53R2), causes severe mitochondrial DNA depletion. Nat Genet 2007;39:776–780.

13. Lane AN, Fan TW. Regulation of mammalian nucleotide metabolism and biosynthesis. Nucl Acids Res 2015;43:2466–2485.

14. Khan N, Shah PP, Ban D, et al. Solution structure and functional investigation of human guanylate kinase reveals allosteric networking and a crucial role for the enzyme in cancer. J Biol Chem 2019;294:11920–11933.

15. Agarwal RP, Scholar EM, Agarwal KC, Parks RE Jr. Identification and isolation on a large scale of guanylate kinase from human erythrocytes. Effects of monophosphate nucleotides of purine analogs. Biochem Pharmacol 1971;20:1341–1354.

16. Hible G, Daalova P, Gilles AM, Cherfils J. Crystal structures of GMP kinase in complex with ganciclovir monophosphate and Ap5G. Biochimie 2006;88:1157–1164.

17. Ionescu MI. Adenylate kinase: a ubiquitous enzyme correlated with medical conditions. Protein J 2019;38:120–133.

18. Panayiotou C, Solaroli N, Karlsson A. The many isoforms of human adenylate kinases. Int J Biochem Cell Biol 2014;49:75–83.

19. Wang L. Mitochondrial purine and pyrimidine metabolism and beyond. Nucleosides Nucleotides Nucl Acids 2016;35:578–594.

20. Di Noia MA, Todisco S, Cirigliano A, et al. The human SLC25A33 and SLC25A36 genes of solute carrier family 25 encode two mitochondrial pyrimidine nucleotide transporters. J Biol Chem 2014;289:33137–33148.

21. Alexander SP, Kelly E, Mathie A, et al. The concise guide to pharmacology 2021/22: transporters. Br J Pharmacol 2021;178:S412–S513.

22. Wang L. Deoxynucleoside salvage enzymes and tissue specific mitochondrial DNA depletion. Nucleosides Nucleotides Nucl Acids 2010;29:370–381.

23. Hidalgo-Gutierrez A, Barriocanal-Casado E, Bakkali M, et al. Beta-RA reduces DMQ/CoQ ratio and rescues the encephalopathic phenotype in Coq9 (R239X) mice. EMBO Mol Med 2019;11:e9466.

24. Pontarin G, Gallinaro L, Ferraro P, et al. Origins of mitochondrial thymidine triphosphate: dynamic relations to cytosolic pools. Proc Natl Acad Sci U S A 2003;100:12159–12164.

25. Hidalgo-Gutierrez A, Barriocanal-Casado E, Diaz-Casado ME, et al. Beta-RA targets Mitochondrial metabolism and adipogenesis, leading to therapeutic benefits against CoQ deficiency and age-related overweight. Biomedicine 2021;9:1457.

26. Gonzalez-Garcia P, Diaz-Casado ME, Hidalgo-Gutierrez A, et al. The Q-junction and the inflammatory response are critical pathological and therapeutic factors in CoQ deficiency. Redox Biol 2022;55:102403.

27. Camara Y, Gonzalez-Vioque E, Scarpelli M, et al. Administration of deoxyribonucleosides or inhibition of their catabolism as a pharmacological approach for mitochondrial DNA depletion syndrome. Hum Mol Genet 2014;23:2459–2467.

28. Landoni JC, Wang L, Suomalainen A. Quantitative solid-phase assay to measure deoxynucleoside triphosphate pools. Biol Methods Protocols 2018;3: bpy011.

29. Minton K. Predicting variant pathogenicity with AlphaMissense. Nat Rev Genet 2023;24:804.

30. Cheng J, Novati G, Pan J, et al. Accurate proteome-wide missense variant effect prediction with AlphaMissense. Science 2023;381: eadg7492.

31. Rath S, Sharma R, Gupta R, et al. MitoCarta3.0: an updated mitochondrial proteome now with sub-organelle localization and pathway annotations. Nucl Acids Res 2021;49:D1541–D1547.

32. Morgenstern M, Peikert CD, Lubbert P, et al. Quantitative high-confidence human mitochondrial proteome and its dynamics in cellular context. Cell Metab 2021;33: 2464–2483.

33. Topalis D, Kumamoto H, Amaya Velasco MF, et al. Nucleotide binding to human UMP-CMP kinase using fluorescent derivatives — a screening based on affinity for the UMP-CMP binding site. FEBS J 2007;274:3704–3714.

34. Lopez-Gomez C, Hewan H, Sierra C, et al. Bioavailability and cytosolic kinases modulate response to deoxynucleoside therapy in TK2 deficiency. EBioMedicine 2019;46:356–367.

35. Lopez-Gomez C, Levy RJ, Sanchez-Quintero MJ, et al. Deoxycytidine and deoxythymidine treatment for thymidine kinase 2 deficiency. Ann Neurol 2017;81:641–652.

36. Markert ML. Purine nucleoside phosphorylase deficiency. Immunodefic Rev 1991;3:45–81.

37. Somech R, Lev A, Grisaru-Soen G, et al. Purine nucleoside phosphorylase deficiency presenting as severe combined immune deficiency. Immunol Res 2013;56:150–154.

38. Taanman JW, Muddle JR, Muntau AC. Mitochondrial DNA depletion can be prevented by dGMP and dAMP supplementation in a resting culture of deoxyguanosine kinase-deficient fibroblasts. Hum Mol Genet 2003;12:1839–1845.

39. Bulst S, Holinski-Feder E, Payne B, et al. In vitro supplementation with deoxynucleoside monophosphates rescues mitochondrial DNA depletion. Mol Genet Metab 2012;107:95–103.

40. Ramon J, Vila-Julia F, Molina-Granada D, et al. Therapy prospects for Mitochondrial DNA maintenance disorders. Int J Mol Sci 2021; 22:6477.

41. Berardo A, Dominguez-Gonzalez C, Engelstad K, Hirano M. Advances in thymidine kinase 2 deficiency: clinical aspects, translational Progress, and emerging therapies. J Neuromuscul Dis 2022;9: 225–235.

42. Amtmann D, Gammaitoni AR, Galer BS, et al. The impact of TK2 deficiency syndrome and its treatment by nucleoside therapy on quality of life. Mitochondrion 2023;68:1–9.

43. Blazquez-Bermejo C, Molina-Granada D, Vila-Julia F, et al. Age-related metabolic changes limit efficacy of deoxynucleoside-based therapy in thymidine kinase 2-deficient mice. EBioMedicine 2019;46: 342–355.

44. An Open-Label Study of Continuation Treatment With Combination Pyrimidine Nucleosides in Patients With TK2 Deficiency (2019) Clinical Trial, (Identification No. NCT03845712) 2019.

45. Treatment of TK2 Deficiency With Thymidine and Deoxycytidine (2018) Clinical Trial (Identification No. NCT03639701), 2018.

46. Dominguez-Gonzalez C, Madruga-Garrido M, Mavillard F, et al. Deoxynucleoside therapy for thymidine kinase 2-deficient myopathy. Ann Neurol 2019;86:293–303.

47. Iino M, Sato T, Nakadate A, et al. Forodesine maintenance therapy for newly diagnosed peripheral T-cell lymphoma: a single-institutional, observational, retrospective analysis. Ann Hematol 2022;101:2351–2352.

48. Bantia S, Miller PJ, Parker CD, et al. Purine nucleoside phosphorylase inhibitor BCX-1777 (Immucillin-H)—a novel potent and orally active immunosuppressive agent. Int Immunopharmacol 2001;1: 1199–1210.

49. Balakrishnan K, Verma D, O'Brien S, et al. Phase 2 and pharmacodynamic study of oral forodesine in patients with advanced, fludarabine-treated chronic lymphocytic leukemia. Blood 2010;116: 886–892.

50. Gandhi V, Balakrishnan K. Pharmacology and mechanism of action of forodesine, a T-cell targeted agent. Semin Oncol 2007;34:S8–S12.